Neuron, Vol. 18, 493–503, March, 1997, Copyright ©1997 by Cell Press

Molecular Determinants of Agonist Discrimination by NMDA Receptor Subunits: Analysis of the Glutamate Binding Site on the NR2B Subunit

Bodo Laube,[†] Hirokazu Hirai,[†‡] Mike Sturgess,[*] Heinrich Betz, and Jochen Kuhse
Department of Neurochemistry
Max-Planck-Institute for Brain Research
Deutschordenstraβe 46
60528 Frankfurt
Federal Republic of Germany
*Symphony Pharmaceuticals Inc.
Frazer, Pennsylvania 19355

Summary

NMDA receptors require both L-glutamate and the coagonist glycine for efficient channel activation. The glycine binding site of these heteromeric receptor proteins is formed by regions of the NMDAR1 (NR1) subunit that display sequence similarity to bacterial amino acid binding proteins. Here, we demonstrate that the glutamate binding site is located on the homologous regions of the NR2B subunit. Mutation of residues within the N-terminal domain and the loop region between membrane segments M3 and M4 significantly reduced the efficacy of glutamate, but not glycine, in channel gating. Some of the mutations also decreased inhibition by the glutamate antagonists, D-AP5 and R-CPP. Homology-based molecular modeling of the glutamate and glycine binding domains indicates that the NR2 and NR1 subunits use similar residues to ligate the agonists' α-aminocarboxylic acid groups, whereas differences in side chain interactions and size of aromatic residues determine ligand selectivity.

Introduction

Glutamate, the major excitatory neurotransmitter in the vertebrate central nervous system, exerts its postsynaptic actions via a diverse set of membrane receptors. Of these, the ionotropic *N*-methyl-D-aspartic acid (NMDA) receptors have gained particular attention because of their crucial roles in brain development, synaptic plasticity, memory formation, and neurotoxicity (Olney, 1990; Nakanishi, 1992). NMDA receptors display a number of unique properties that distinguish them from other ligand-gated ion channels. First, NMDA receptor channels are blocked by extracellular Mg^{2+} at resting membrane potential and open only upon simultaneous depolarization and agonist binding (Mayer et al., 1984). Second, NMDA receptor channels are highly permeable to monovalent ions and Ca^{2+} (Mayer and Westbrook, 1987). NMDA receptor-mediated Ca^{2+} entry triggers important cellular processes, including changes in synaptic efficacy, such as long-term potentiation and heterosynaptic depression (Madison, 1991), and prolonged stimulation resulting in high Ca^{2+} influx causes neuronal cell death in ischemia and other neurodegenerative disorders (Choi, 1988). Third, simultaneous binding of glutamate and the coagonist glycine is required for efficient activation of NMDA receptors (Johnson and Ascher, 1987; Kleckner and Dingledine, 1988). The mechanism of coagonist action is not entirely clear but may involve allosteric modulation of agonist binding affinities (Mayer et al., 1989). Pharmacological and electrophysiological studies indicate that glutamate and glycine occupy distinct sites of the receptor protein (Reynolds et al., 1987; Henderson et al., 1990).

Molecular studies have shown that NMDA receptors are oligomeric membrane proteins composed of homologous NMDAR1 (NR1) and NR2 subunits (reviewed by Hollmann and Heinemann, 1994). The NR1 and NR2 subunits are synthesized as precursor proteins with a cleavable leader sequence followed by a long N-terminal extracellular domain and, in the second half of the polypeptides, four hydrophobic membrane segments (M1–M4). The M1, M3, and M4 segments are transmembrane spanning, whereas segment M2 is thought to form a reentrant loop (Hollmann and Heinemann, 1994; Bennett and Dingledine, 1995; Wo and Oswald, 1994; Hirai et al., 1996) that lines the ion channel (Kuner et al., 1996). The NR1 subunit is expressed in several distinct splice variants throughout the central nervous system (Durand et al., 1992; Nakanishi et al., 1992; Sugihara et al., 1992; Hollmann et al., 1993). The NR2 subunit exists in four isoforms encoded by different genes (NR2A-D), which create further functional and regional heterogeneity of NMDA receptors (Kutsuwada et al., 1992; Meguro et al., 1992; Monyer et al., 1992). Heterologous expression in Xenopus laevis oocytes has suggested that the NR1 subunit can form channels that are activated upon coapplication of glutamate and glycine (Moriyoshi et al., 1991; Durand et al., 1992). However, in mammalian cell lines, functional channels are not detected upon expression of NR1 alone (Grimwood et al., 1995; McIlhinney et al., 1996). Coexpression of the NR1 and an NR2 subunit, in contrast, reproducibly creates large current responses in both expression systems (Kutsuwada et al., 1992; Meguro et al., 1992; Monyer et al., 1992). This is consistent with a hetero-oligomeric structure of NMDA receptors.

Site-directed mutagenesis has identified determinants of glycine binding in distinct regions of the NR1 subunit (Kuryatov et al., 1994; Wafford et al., 1995; Hirai et al., 1996). Their localization is consistent with a model of the glycine-binding pocket, in which the coagonist is bound by a "Venus' flytrap" mechanism between two domains formed by a sequence preceding the first membrane segment M1 and the loop separating membrane segments M3 and M4, respectively (Kuryatov et al., 1994; Hirai et al., 1996). Interestingly, these regions of glutamate receptor proteins display significant sequence similarity with a family of bacterial amino acid–binding proteins (Nakanishi et al., 1990; O'Hara et al., 1993), suggesting that a phylogenetically conserved amino acid–binding fold (Oh et al., 1993) creates the

[†] These authors contributed equally to this work.
[‡] Present address: Laboratory for Synaptic Function, Frontier Research Program, The Institute for Physical and Chemical Research RIKEN, Wako, Saitana 351–01, Japan.

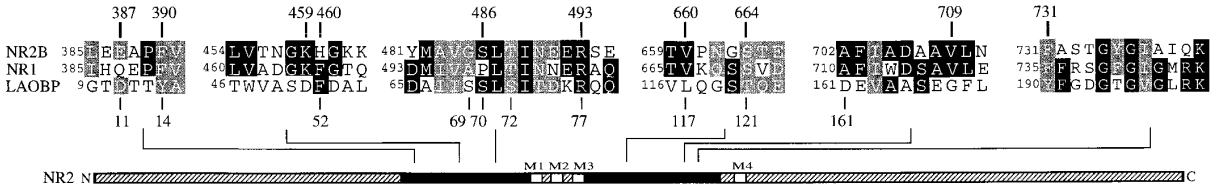

Figure 1. Partial Alignments of NMDA Receptor Subunit Homology Regions with LAOBP

Regions of the NR2B subunit (Kutsuwada et al., 1992) are aligned with the corresponding sequences of NR1 (Moriyoshi et al., 1991) and the bacterial periplasmic protein LAOBP (Kang et al., 1991). Identical residues are indicated by black boxes, and isofunctional residues are denoted by gray boxes. Amino acid substitutions of NR2B are indicated above the alignment, and residues of LAOBP crucial for ligand binding are given below the respective sequence. The relative positions of the identified binding motifs are shown in a schematic representation of the NR2B polypeptide. The positions of the first residue of each partial sequence are indicated.

binding pockets of diverse types of glutamate receptors. Indeed, swapping of the respective domains has allowed to inverse the pharmacology of recombinant α-amino-3-hydroxy-5-methyl-4-isoxazolepropionate (AMPA) and kainate receptor proteins (Stern-Bach et al., 1994). In addition, expression of soluble fusion constructs encompassing these regions of the GluR2 and GluR4 glutamate receptor subunits in eukaryotic cells or bacteria resulted in proteins displaying the binding pharmacology of AMPA and kainate receptors (Kuusinen et al., 1995; Arvola and Keinänen, 1996).

In this study, we have analyzed these homology regions in the NR2B subunit by substituting residues corresponding to positions mediating glycine binding to the NR1 protein, and we show that they are crucial for glutamate activation of the NMDA receptor. Our data reveal positional identity of the determinants of glutamate binding to the NR2B subunit and those of glycine binding to the NR1 protein. Molecular modeling of the respective domains of the NR1 and NR2B subunits into the known coordinates of the bacterial leucine–arginine–ornithine binding protein (LAOBP) from Salmonella typhimurium (Oh et al., 1993) provides structures that shed light on the pharmacological specificity of agonist and antagonist binding to the NMDA receptor. Our data create an experimental basis for rationalizing the design of novel NMDA receptor ligands, which could serve as therapeutic tools for preventing excitotoxic NMDA receptor activation in different acute and chronic neurodegenerative disorders.

Results

Major Determinants of Glutamate Binding Are Localized in the N-Terminal Extracellular Domain of the NR2B Subunit

To determine whether amino acid residues within NR2 subunits are involved in ligand binding, we introduced substitutions into the NR2B subunit at positions homologous to those in the NR1 protein that are known to be important for glycine binding (Kuryatov et al., 1994; Wafford et al., 1995; Hirai et al., 1996). The mutated residues are localized in the two domains of the NR2 polypeptide that show sequence and structural homology with periplasmic bacterial amino acid–binding proteins, in particular LAOBP (O'Hara et al., 1993), e.g., the domain preceding membrane segment M1 and the loop between membrane segments M3 and M4 (Figure 1). This loop is known to be localized extracellularly in AMPA–kainate receptors (reviewed by Wo and Oswald, 1995) and the NR1 subunit (Hirai et al., 1996). The mutant NR2B subunits then were coexpressed with the NR1 subunit in Xenopus laevis oocytes, and dose-response relations for glycine and glutamate were established by voltage-clamp recording.

As shown in Figure 2, ion flux through the NR1–NR2B wild-type receptor in the presence of a saturating concentration of glutamate was maximal at glycine concentrations between 1–10 μM, whereas saturation of the glutamate response in the presence of glycine occurred at 10–100 μM; the corresponding concentrations for half-maximal activation (EC_{50}) were 0.54 and 1.5 μM, respectively (Table 1). A significant difference in glutamate affinity was found for two substitutions ($NR2B^{E387A}$ and $NR2B^{F390S}$) corresponding to the most N-terminal glycine-binding residues of the NR1 subunit (Kuryatov et al., 1994). Whereas the dose-response curves for glycine showed EC_{50} values similar to that of the wild-type receptor, the EC_{50} values for glutamate were increased about 240-fold for $NR2B^{E387A}$ and 50-fold for $NR2B^{F390S}$, respectively (Figures 2 and 3). Maximal current flow (I_{max}) was not impaired in the $NR2B^{E387A}$ mutant but was reduced about 10-fold in mutant $NR2B^{F390S}$ (Table 1). These data are consistent with the NR2B subunit having a crucial role in glutamate binding.

To further delineate contributions of the NR2B subunit to the glutamate binding site of the NMDA receptor, another set of substitutions was analyzed. First, we mutated the basic residues K459 and H460 (Figure 1); these amino acids correspond to a conserved motif in the ligand binding site of glutamate receptors, including the NR1 subunit (Kuryatov et al., 1994; Wafford et al., 1995), the GluR1 subunit (Uchino et al., 1992), and the chick kainate binding protein (Paas et al., 1996a). Introduction of a negatively charged glutamate side chain in mutant $NR2B^{K459E}$ resulted in a 180-fold increased EC_{50} value for glutamate (Figures 2 and 3 and Table 1) but had no significant effect on glycine affinity. Similarly, substitution of the neighboring histidine residue by phenylalanine in mutant $NR2B^{H460F}$ caused a selective decrease in glutamate affinity without changing the glycine response (Table 1). A third region contributing to glutamate binding was identified in a region preceding segment M1. Coexpression of mutant $NR2B^{S486A}$ with the NR1 subunit generated NMDA receptors that displayed an EC_{50} value for glutamate of 65 μM, without a detectable change in apparent glycine affinity (Figure 3). Isofunctional replacement of an arginine residue ($NR2B^{R493K}$) within the

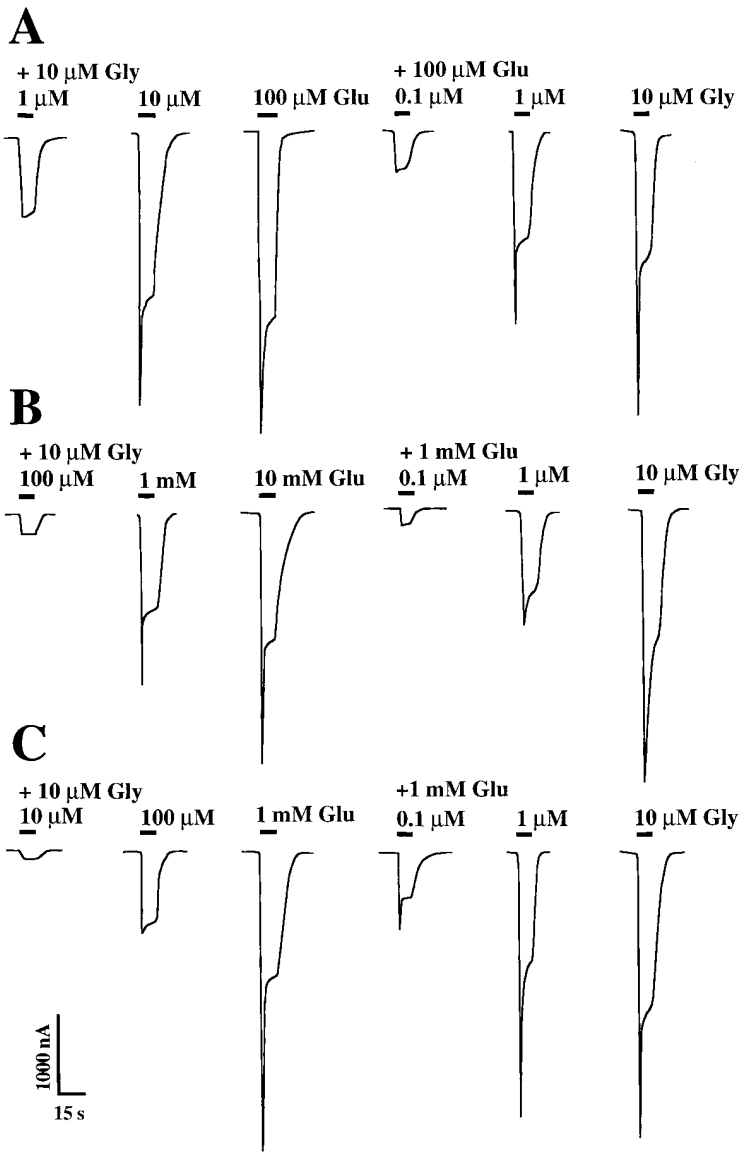

Figure 2. Agonist Response Properties of Wild-Type and Mutant NR2B Subunits

In vitro transcribed wild-type or mutant NR2B subunit cRNAs were coinjected with the NR1 subunit cRNA into defolliculated Xenopus oocytes. Membrane currents elicited by superfusion of increasing concentrations of glutamate in the presence of 10 μM glycine (left) or of increasing concentrations of glycine in the presence of 0.1–1 mM glutamate (right) were recorded 2–6 days after injection. Traces obtained with the wild-type NR2B subunit (A), mutant NR2B^{E387A} (B), and mutant NR2B^{K459E} (C) are shown.

same region resulted in a complete loss of the agonist response (Table 1). In conclusion, residues close to membrane segment M1 of the NR2B subunit seem to be important for glutamate binding to and/or channel function of the NMDA receptor.

The M3–M4 Loop Region of the NR2B Subunit Contributes to Glutamate Binding

In the NR1 subunit, proximal and distal residues of the extracellular M3–M4 loop are known to contribute to coagonist potentiation of the NMDA receptor (Kuryatov et al., 1994; Hirai et al., 1996). Therefore, agonist dose-response curves were established for mutants NR2B^{V660A} and NR2B^{S664G}. These mutations are located in a region homologous to the proximal portion of the glycine binding domain in the M3–M4 loop region of the NR1 subunit (Figure 1). Replacement of V660 by alanine resulted in an ≈20-fold increase in the EC_{50} value for glutamate, whereas substitution of S664 increased the latter >100-fold (Figure 3 and Table 1). A substitution in a distal region of sequence homology between NMDA receptor subunits and LAOBP similarly affected the apparent affinity of glutamate: mutant NR2B^{V709A} displayed a 30-fold increased EC_{50} value for glutamate activation (Figure 3). None of these mutants showed a significant change in the EC_{50} value of glycine (Table 1). Substitution of F731, a residue homologous to F735 in the C-terminal part of the M3–M4 loop of the NR1 subunit (Hirai et al., 1996), in mutant NR2B^{F731A} failed to alter the glutamate response of the receptor; however, similar to the results obtained with NR2B^{F390A}, a significant reduction in maximal current was observed (Table 1).

Glutamate Antagonist Sensitivity of the NR2B Mutants

The data reported above indicate that major determinants of glutamate binding are localized on the NR2B subunit. To corroborate this finding further, we investigated whether the substitutions introduced affected the potency of specific glutamate antagonists. To this end,

Table 1. Glutamate and Glycine Response Properties of the NR2B Mutants

	EC_{50} [μM]			
	L-Glutamate	Glycine	I_{max} [μA]	n
NR2B	1.5 ± 0.6 (1.6)	0.54 ± 0.27 (1.7)	3.8 ± 1.2	8
E387A	355 ± 74* (1.5)	0.82 ± 0.37 (1.5)	3.1 ± 0.5	6
F390S	71 ± 23* (1.5)	0.91 ± 0.42 (1.5)	0.31 ± 0.18	8
K459E	270 ± 68* (1.4)	0.28 ± 0.13 (1.7)	3.1 ± 0.9	7
H460F	13 ± 6.3* (1.1)	0.33 ± 0.24 (1.8)	4.2 ± 0.7	6
S486A	65 ± 17* (1.4)	0.51 ± 0.31 (1.5)	3.7 ± 1.6	10
R493K	NF	NF	0	20
V660A	27 ± 8.2* (1.5)	0.79 ± 0.26 (1.7)	1.3 ± 0.6	8
S664G	177 ± 64* (1.2)	0.82 ± 0.38 (1.7)	2.2 ± 1.0	9
V709A	41 ± 16* (1.7)	1.0 ± 0.1 (1.8)	3.3 ± 1.3	8
F731A	1.1 ± 0.3 (1.4)	1.3 ± 0.2* (1.2)	0.74 ± 0.36	4

Wild-type and mutant NR2B cRNAs were coinjected with the NR1a cRNA into *Xenopus* oocytes, and the receptors generated were analyzed by voltage-clamp recording as detailed under Experimental Procedures. EC_{50} values ± SD were calculated from dose-response curves obtained from 3–9 oocytes; the respective Hill coefficients (n_H) are given in brackets. Nonfunctional mutants were tested in ≥20 oocytes. I_{max} values were determined in the presence of saturating concentrations of L-glutamate and glycine, respectively. EC_{50} values marked by an asterisk were significantly different ($p < 0.01$) from those of the wild-type receptor. NF, nonfunctional; n, number of experiments.

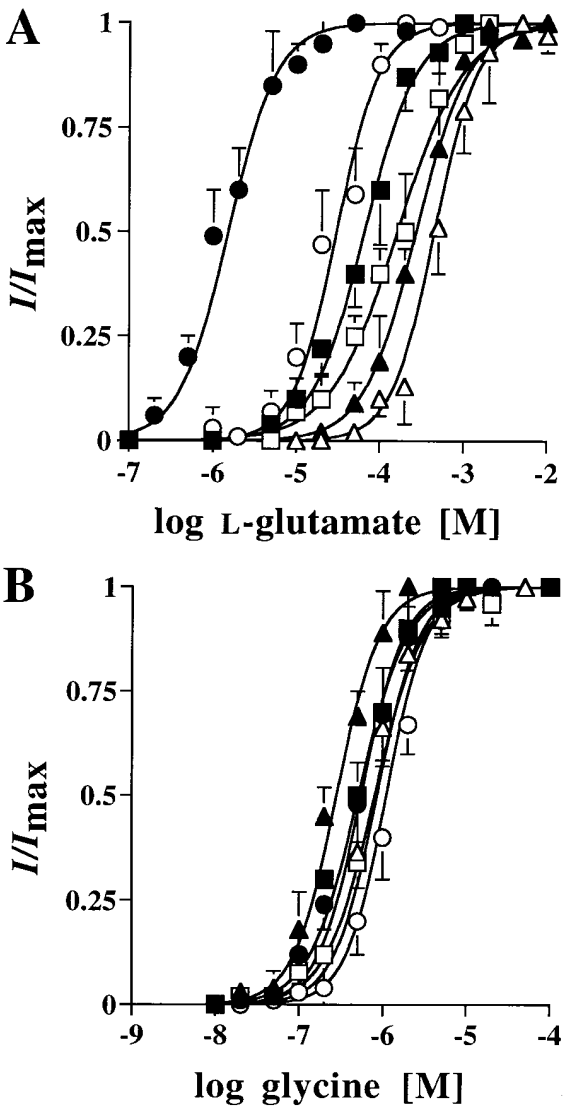

Figure 3. Agonist Dose-Response Curves of Wild-Type and Mutant NR2B Subunits

Dose-response curves for glutamate in the presence of saturating concentrations of glycine (A) and for glycine in the presence of saturating concentrations of glutamate (B) were determined for the wild-type NR2B (closed circles) and the mutant $NR2B^{E387A}$ (open triangles), $NR2B^{K459E}$ (closed triangles), $NR2B^{S486A}$ (closed squares), $NR2B^{S664G}$ (open squares), and $NR2B^{V709A}$ (open circles) subunits. For EC_{50} values and Hill coefficients, see Table 1.

inhibition curves were established at glutamate concentrations corresponding to the EC_{50} values of the respective NR2B mutants in the presence of saturating glycine concentrations (Figure 4). Half-maximal inhibition was seen for the phosphonic acid derivative D-(-)-2-amino-5-phosphonopentanoic acid (D-AP5) at a concentration of ≈4.7 μM with the wild-type NR2B subunit (Table 2). A 40-fold increase in the concentration required for half-maximal inhibition (IC_{50}) was obtained with mutant $NR2B^{K459E}$, where an IC_{50} value of 190 μM was determined (Figure 4). Simultaneously, the sensitivity for a another related antagonist, 3-((*R*)-2-carboxypiperazin-4-yl)-propyl-1-phosphonic acid (R-CPP), was reduced 8-fold for the same mutation (Table 2). In addition, significant reductions in D-AP5 inhibition were obtained for mutants $NR2B^{S486A}$, $NR2B^{S664G}$ and $NR2B^{V709A}$ (Figure 4 and Table 2). Thus, common binding determinants are shared by agonists and antagonists of the glutamate site of the NMDA receptor.

Molecular Modeling of the Glutamate and Glycine Binding Sites

The mutational analysis presented above shows that substitutions in NR2B at positions homologous to the glycine binding residues of the NR1 subunit increase the concentrations of glutamate, but not glycine, required for NMDA receptor channel gating. This is consistent with a conserved architecture of the agonist binding folds formed by the NR1 and NR2 subunits. Based on homology considerations, we previously proposed a bilobate structure of the glycine binding site of the NR1 subunit that used the known crystal structure of LAOBP as a template (Kuryatov et al., 1994; Hirai et al., 1996). Here, we evaluated our data from mutational analysis further by modeling the glutamate and glycine binding sites of the NMDA receptor at high resolution. The N-terminal homology segments and most of the M3–M4 sequence could be adequately fitted into the known coordinates of lobes I and II of LAOBP (Oh et al., 1993). However, to conserve three α-helical regions characteristic of LAOBP's amino acid–binding site, a slightly modified version (see Figure 1) of previous alignments of the NR2B and NR1 sequences with LAOBP (Monyer et al., 1992; Kuryatov et al., 1994; Hirai et al., 1996) had to be used. It should be emphasized that our binding site models represent the liganded states of these proteins before closure according to the "Venus' flytrap" model. We choose to model these states because they are likely

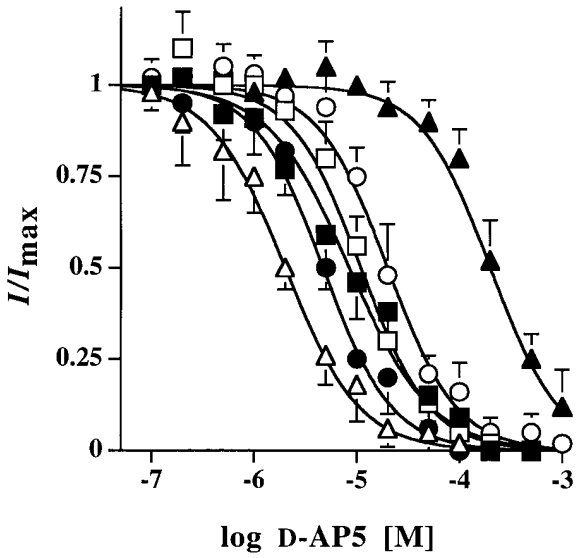

Figure 4. Inhibition of NR2B Wild-Type and Mutant Glutamate Responses by D-AP5

Antagonist dose-response curves obtained with oocytes injected with wild-type NR2B (closed circles), NR2B^{E387A} (open triangles), NR2B^{K459E} (closed trianges), NR2B^{S486A} (closed squares), NR2B^{S664G} (open squares), and NR2B^{V709A} (open circles) cRNAs are shown. The glycine concentrations used were 10 μM for the wild-type and the mutated NR2B subunits. Glutamate was used at concentrations eliciting a half-maximal response as determined (Table 1). Data are plotted as a fraction of the current observed in the absence of antagonist. For IC_{50} values, see Table 2.

to represent the conformations from which the reactions leading to channel opening are initiated and thus are most relevant to NMDA receptor pharmacology. Receptor–ligand interactions were modeled employing these "open" binding site configurations by using unconstrained minimization. As a consequence, interacting residues on lobe II may appear more distant in our models than predicted for the closed ligated proteins.

Table 2. Inhibition of Current Responses by Glutamate Antagonists

	IC_{50} [μM]	
	R-CPP	D-AP5
NR2B	0.92 ± 0.36 (4)	4.7 ± 1.3 (4)
E387A	0.83 ± 0.24 (6)	1.5 ± 0.6 (3)
F390S	0.76 ± 0.31 (3)	3.9 ± 2.5 (3)
K459E	7.8* ± 2.9 (3)	190* ± 24 (3)
H460F	1.1 ± 2.7 (5)	7.3 ± 1.0 (3)
S486A	2.1* ± 0.3 (4)	8.7* ± 2.2 (5)
V660A	2.4 ± 1.3 (5)	4.4 ± 0.6 (3)
S664G	1.2 ± 0.5 (6)	11* ± 2.4 (3)
V709A	0.69 ± 0.31 (3)	28* ± 12 (3)
F731A	1.9 ± 0.4 (3)	7.4 ± 3.6 (3)

Wild-type or mutant NR2B subunits were coexpressed with the NR1a polypeptide, and current responses were analyzed by voltage-clamp recording as detailed under Experimental Procedures. IC_{50} values were determined at the EC_{50} value of L-glutamate in the presence of saturating concentrations of glycine for 3–6 oocytes each. The Hill coefficients for R-CPP and D-AP5 inactivation were n_H = 1.0–1.4 and 1.0–1.2, respectively, for the wild-type NR2B subunit and all mutants tested. Values indicated by stars are significantly different from wild-type (p = 0.01). Numbers in brackets (n) indicate the number of experiments performed.

The Glutamate Binding Pocket of the NR2B Subunit

The surface structure of the region of NR2B harboring the glutamate binding fold is displayed in Figure 5A. The predicted agonist binding site resides within a cleft formed by the two homology regions that can accommodate ligands larger than glutamate. Modeling of glutamate into this pocket revealed that an optimal orientation of L-glutamate can be achieved when the α-carboxyl group of the ligand is allowed to interact with R493 and T488 (Figure 5B). The α-amino group of the ligand then is hydrogen bonded to E387 and the backbone carbonyl group of S486 (Figure 5B). These two residues contribute to a ring of hydrophilic amino acids (including E387, H460, S486, T488, and R493) at the bottom of the binding pocket that overlie a layer of hydrophobic side chains (Figure 5B). The γ-carboxyl group of glutamate is predicted to lie in the vicinity of, but not in direct contact with, two regions of the receptor surface that contain charged residues, e.g., K463 adjacent to residue E492 (Figure 5B), and N490 adjacent to R667 (not shown). Assuming that K463 and R667 are in the protonated state, these residues may form the center of an electron-deficient patch that attracts the γ-carboxyl group of glutamate (Figure 5A). S664 lies at the upper edge of this electron-deficient patch and may contribute to the stabilization of the positively charged residues K463 and R667 (not shown) via the γ-carboxyl group of the ligand (Figure 5B). In accordance with our findings, substitution of this residue should disrupt the polar surface in this region of the binding pocket (see Figure 5A) and thus lower glutamate affinity. Since S664 is part of the upper surface of the "Venus' flytrap"-like structure, a tighter interaction between S664 and the agonist may occur upon closure of the binding pocket. Another critical lysine residue, K459, is situated at its lower left edge (behind the amino group of glutamate in our projection; therefore not shown); mutation NR2B^{K459E} drastically lowered the EC_{50} value of glutamate. Our model indicates that the charged side chain of K459 interacts with E386 and E417, thus stabilizing the electron-rich portion of the agonist binding pocket without directly interacting with the ligand. This stabilization is disrupted upon introducing a side chain of opposite charge.

To unravel features of L-glutamate that enable this ligand to bind in an agonistic fashion, we also modeled the interaction with the antagonists tested above, D-AP5 (Figure 5C) and R-CPP (not shown). Both compounds represent elongated analogs of glutamate, in which the γ-carboxyl group is replaced by a phosphonic acid moiety. While such acids may be in equilibrium with the monoanionic form, we chose the fully ionized species for modeling in order to simplify the search of conformation space available for each ligand. Additionally, the second nitrogen atom of R-CPP was evaluated in a protonated state. The resulting ligand–receptor models predict that the α-aminocarboxylic acid portions of the antagonists adopt an orientation similar to that of L-glutamate. The α-carboxyl group is hydrogen bonded between T488 and R493, while the adjacent protonated nitrogen center is stabilized by E387 (shown for D-AP5 in Figure 5C).

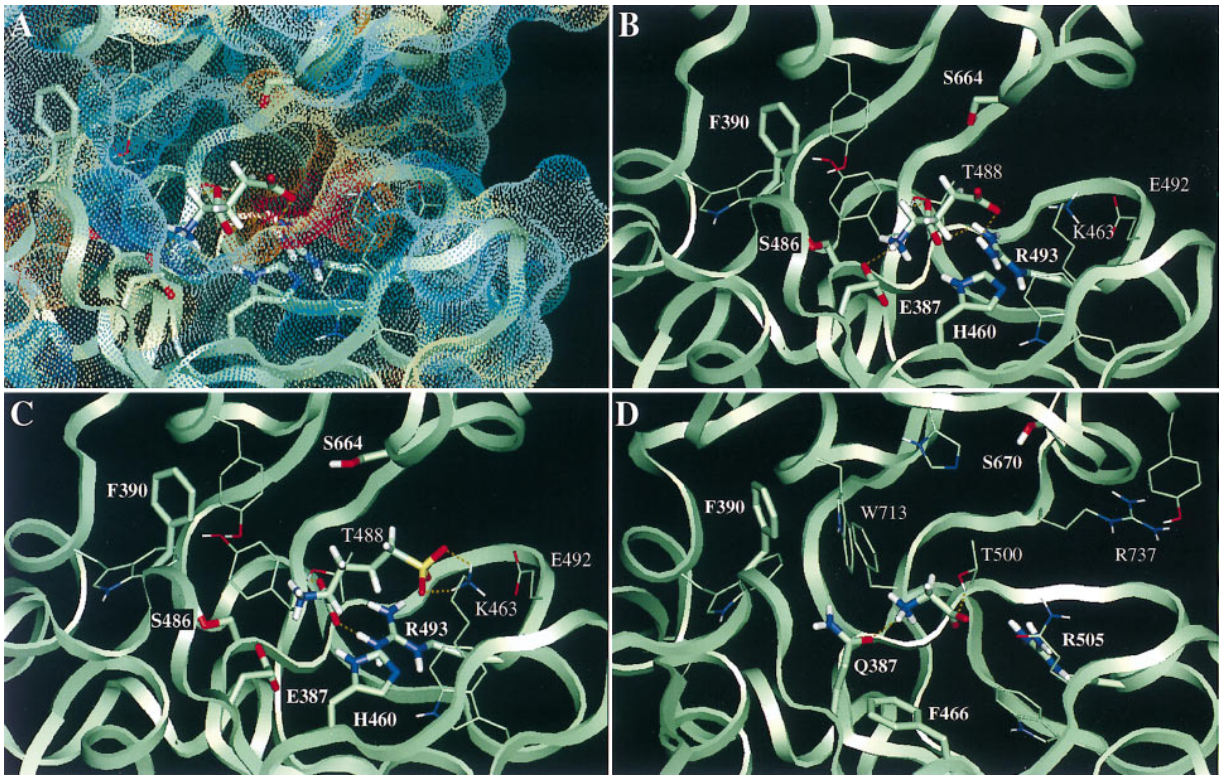

Figure 5. Models of the Glutamate and Glycine Binding Sites of the NMDA Receptor

(A) Electron density surface and ribbon representation of the vicinity of the binding pocket of the NR2B subunit ligated with glutamate. The structure of glutamate is displayed as a stick model. The peptide backbone is indicated by a white ribbon. Carbon atoms are shown in gray, oxygen in red, nitrogen in blue, and hydrogen in white. Note electron-deficient surface (in red) of the region of the binding pocket underlying glutamate's γ-carboxyl group; blue regions represent areas of high electron density.

(B) Close-up view of the binding pocket of the NR2B subunit ligated with glutamate. Binding residues identified by site-directed mutagenesis are shown in bold letters, whereas residues predicted to contribute to ligand binding by molecular modeling are indicated in plain text. Predicted side chain interactions of glutamate are indicated by dashed lines. The α-amino group of glutamate is hydrogen bonded to E387 and the backbone carbonyl group of S486; the α-carboxyl group interacts with R493 and T488. The γ-carboxyl group of glutamate forms a salt bridge with R493 and can interact with K463 and R667 (not shown), which binds to S664.

(C) Structure of the NR2B binding pocket, ligated with D-AP5. The α-aminocarboxylic acid portion of the antagonist is ligated similarly as that of glutamate in (B). The phosphonic acid head group closely interacts with U463. (The viewing angle of this display differs slightly from that in [B] in order to improve visualization of the bound antagonist.)

(D) Model of the binding pocket of the NR1 subunit ligated with glycine. Note that the overall structure of the binding pocket and the arrangement of binding residues are very similar to those of NR2B (B). The carboxyl group of glycine interacts with R505 and T500, whereas the amino group is hydrogen bonded to Q387 (and the backbone carbonyl group of P498; not shown).

Owing to the greater side chain lengths of these ligands, the terminal phosphonic acid groups can directly hydrogen bond to K463 without perturbing the side chain geometry of this residue (Figure 5C).

The Glycine Binding Pocket of the NR1 Subunit

The structure of the glycine binding pocket obtained by identical procedures through modeling of the NR1 homology regions shares many features with that of the glutamate binding site. Again, an arginine residue (R505) together with a threonine (T500) ligates the carboxyl group of glycine (Figure 5D). T500 is embedded in a sequence (positions 497–502) similar to that described above for the NR2B subunit, which is predicted to form a loop prior to the third helical region and to line the bottom of the binding pocket (not shown). Consistent with our mutagenesis data, the amino group of glycine is hydrogen bonded to Q387 (Figure 5D) and to the backbone carbonyl group of P498 (not shown). F466 appears to stabilize the amino group of the bound ligand and R505. The upper region of the binding pocket contains a series of tryptophan and histidine residues (Figure 5D and not shown). The aromatic residues F390 and W713 may form some type of zipper along one end of the pocket structure, which could participate in the opening and closing of the binding fold similar to that of LAOBP (Oh et al., 1993). Mutation of F390 may prevent the underlying conformational transition and thus explain the effects of respective substitutions on glycine coagonism (Kuryatov et al., 1994).

We also examined the binding of glycine site antagonists into the binding pocket of the NR1 subunit (data not shown). Both 7-chlorokynurenate and its extended high affinity derivative, L701,324, were chosen as representative competitive inhibitors of this site (Kemp and Leeson, 1993). The electron-rich 2-quinolone carbonyl unit of both ligands appeared to interact with R505,

while the chloroaromatic ring filled the left side of the binding pocket, where it may be involved in π-electron interactions with the numerous aromatic residues that occupy this side of the NR1 binding pocket, in particular F466. Interestingly, the phenoxyphenyl side chain of L701,324 seemed to stabilize both R505 and also the distant R737 (Figure 5D). The latter residue is close to a pair of phenylalanines (F735 and F736, not shown), which are crucial for glycine activation of the NMDA receptor (Hirai et al., 1996).

In conclusion, although the sequences of the glutamate and glycine binding sites differ by residue changes that imply differential adjustments of backbone residues, both agonist binding pockets appear to be remarkably similar in their overall structures despite their rather differently sized ligands. Apart from individual side chain substitutions, major structural differences seem to involve the presence of more bulky aromatic residues in the amino group binding region of the NR1 pocket, compared to the NR2 glutamate binding site.

Discussion

The data presented in this study indicate that major determinants of glutamate binding to the NMDA receptor reside in the extracellular domains of NR2 subunits. Although our experiments focused on the NR2B polypeptide, it should be emphasized that the binding residues identified here are strictly conserved in all NR2 subunits. The location of the glutamate binding site on the NR2 subunits is surprising in view of the initial isolation of the NR1 subunit cDNA by expression cloning in Xenopus laevis oocytes of channels that are cooperatively gated by glutamate and glycine (Moriyoshi et al., 1991). Furthermore, different studies have reported the formation of functional NMDA receptors upon injection of NR1 cRNA into oocytes (Durand et al., 1992; Hollmann et al., 1993; Zheng et al., 1994). However, these homomeric receptors form only with low efficiency and display unusual properties not detectable in native receptors, like a potentiation by micromolar concentrations of Zn^{2+} (Hollmann et al., 1993) and a resistance to redox modulation (Sullivan et al., 1994). Furthermore, expression of the NR1 subunit cDNA alone does not generate glutamate-gated ion channels in mammalian cell lines; here, coexpression of the NR1 with an NR2 subunit is essential for obtaining functional NMDA receptors (Grimwood et al., 1995; Priestley et al., 1995; McIlhinney et al., 1996). This suggests that Xenopus oocytes may contain proteins, e.g., chaperones or endogenous NR2-like subunits, which are essential for the assembly of functional recombinant NMDA receptors. Radioligand binding studies with mammalian cells expressing the NR1 subunit have confirmed the presence of a high affinity glycine binding site on this polypeptide, whereas neither NMDA nor the competitive glutamate antagonist [^{3}H]CGP-39653 bound under the same conditions (Laurie and Seeburg, 1994; Lynch et al., 1994; Grimwood et al., 1995; Kawamoto et al., 1995). In one report, high affinity [^{3}H]glutamate binding to the NR1 subunit expressed in HEK 293 cells has been detected; however, this binding resisted displacement by NMDA or antagonists, thus questioning the functional relevance of this site (Laurie und Seeburg, 1994). Pharmacologically specific high affinity binding of glutamate and NMDA has, however, recently been demonstrated to the singly expressed NR2A subunit, confirming that NR2 proteins are sufficient to form a proper glutamate binding site (Kendrick et al., 1996). In conclusion, these and our mutagenesis data are consistent with the glycine and glutamate binding sites residing on different subunits of the NMDA receptor, the NR1 and the NR2 proteins, respectively. Allosteric interactions between these subunits may explain the differences observed in glycine binding affinities when coexpressing the NR1 with different NR2 subunit isoforms (Monyer et al., 1992; Kendrick et al., 1996).

Our data on mutant NR2B subunit expression support a strict segregation of the glutamate and glycine binding sites to the different NMDA receptor polypeptides. Substitution of NR2B residues in the region preceding membrane segment M1 and the loop domain separating membrane segments M3 and M4 caused drastic decreases in the apparent affinity for glutamate without significantly changing the glycine response. Inversely, mutation of the corresponding regions of the NR1 subunit has been shown to strongly reduce the potency of glycine, but not of glutamate, in channel gating (Kuryatov et al., 1994; Hirai et al., 1996). Since two molecules of glutamate and glycine each are thought to be required for channel activation (Benveniste and Mayer, 1991; Clements and Westbrook, 1991), this implies that the NMDA receptor should be composed of at least four subunits. Indeed, recent data from our laboratory suggest that heteromeric NR1–NR2B receptors have a tetrameric structure (B. L., J. K., and H. B., unpublished data). In both subunits, the mutated regions display significant sequence and structural homology to bacterial amino acid–binding proteins, indicating the conservation of an ancestral amino acid–binding fold within NMDA receptor polypeptides (O'Hara et al., 1993). Using this sequence homology and the known three-dimensional structure of LAOBP, we modeled the glutamate and glycine binding sites of the NR2B and NR1 subunits, respectively, at high resolution. Our models reveal that both agonist binding sites are rather similar in their overall structures but differ in some crucial side chains and size of aromatic residues. The arrangement of these substitutions provides an explanation for the high selectivity of agonist and antagonist binding by these subunits.

The most significant changes of apparent glutamate affinities were obtained with mutations within three short sequence regions of the NR2B subunit. In particular, substitution of E387, K459, and S664 resulted in a 100 to $>$200-fold decrease of glutamate affinity. Our model of the glutamate binding site predicts that replacement of E387 by alanine causes a loss of the ionic interaction with the agonist's α-amino group. In contrast, K459 does not appear to interact directly with bound glutamate but might have a crucial role in stabilizing the ligand binding pocket. R493 seems to be particularly important for glutamate binding since replacement of this residue in the NR2B subunit by an isofunctional lysine residue resulted in the formation of a nonfunctional receptor. A similar result has previously been obtained upon mutation of the homologous positions in the NR1 subunit (Hirai et

al., 1996) and the GluR1 polypeptide (Uchino et al., 1992). Our homology-based modeling of the NR2B and NR1 binding folds reveals that this conserved arginine extends its side chain from a highly conserved helix directly toward the ligand. Thus, in analogy to the homologous R77 of LAOBP (Oh et al., 1993), the guanidinium groups of R493 in the NR2B subunit and of R505 in the NR1 subunit interact ionically with the α-carboxyl groups of glutamate and glycine, respectively.

In contrast to these highly conserved structures ligating the α-aminocarboxylic acid portion of the agonists, the residues contacting the agonist side chains diverge between NR1 and NR2. In particular, the positively charged ring system of H460 in the NR2B subunit appears to be crucial for the high affinity binding of glutamate. In the NR1 subunit, the residue equivalent to H460 corresponds to F466. This may reflect differences in the hydrophilic nature of the agonist side chains and the residues at position 387 (glutamate in NR2B versus glutamine in NR1, respectively). While both of the latter residues could act as π-electron donors for stabilization to the ligand's protonated α-amino group, the additional hydrophilicity of the histidine ring might provide further stabilization of the more polar NR2B binding pocket. Replacement of S664 by glycine resulted in a significant reduction of glutamate affinity; this is consistent with the close apposition of this residue to the extended side chain of glutamate. In contrast, mutation of the homologous S670 of the NR1 subunit had no effect on glycine affinity, which agrees well with the considerable distance between this residue and the bound agonist.

Comparison of the models of NR2B ligated by the competitive glutamate antagonists D-AP5 and R-CCP with that of the glutamate-occupied binding site corroborates the above-mentioned conclusions. The α-carboxyl group of these phosphonic acid–based antagonists is predicted to be stabilized by T488 and R493, while the protonated α-amino group forms a salt bridge with E387. Although, in contrast to glutamate, both antagonists exhibit an R stereochemistry around the C2 center, the stabilization of this portion of all ligands is highly comparable. Thus, residues E387, F390, H460, S486, and R493 form a common binding motif for the α-aminocarboxylic acid region of glutamate and its structurally related antagonists. In contrast, the interactions of the phosphonic acid side chains with the binding pocket differ from that of glutamate. While the side chain of L-glutamate is not long enough to form a strong hydrogen bond with the positively charged head group of K463, D-AP5 and R-CPP strongly interact with this lysine. The longer side chains of these antagonists also imply that the phosphonic acid groups are not in close proximity to S664, which is consistent with the modest effect of the S664A mutation on antagonist affinity. In conclusion, K463 and S664 appear to be crucial determinants of a second binding motif that is important for agonist–antagonist discrimination.

While our models predict that the interactions of L-glutamate and phosphonic acid antagonists with the NR2B glutamate binding pocket are very similar, the results of mutations within the α-aminocarboxylic acid binding region (E387, F390S, K459E, and H460F) appear to suggest the contrary. We interprete this discrepancy to indicate that for efficient agonistic binding, the two ends of glutamate must be bound by the receptor surface. This may be attained by a conformational change within the receptor pocket, which reduces the distance between the two binding motifs identified in this study. We propose that this conformational change is only induced by agonists. Conversely, a simple antagonist acts by blocking the binding motifs without altering their distance. Accordingly, activation of the ion channel complex results from an allosteric motion of the subunits initiated by contraction of the distance between the two regions of the binding fold that interact strongly with L-glutamate. The highly provocative positioning of K463 close to the exterior of the binding pocket and its charge pairing with the surface-exposed acidic side chain of E492 suggest that these residues may be crucial in transmitting the "signal" of glutamate binding to the surface of the individual NR2B subunit, thus triggering opening of the oligomeric ion channel complex. Specifically, a relocation of K463 toward the γ-carboxyl group of the bound agonist may initiate the chain of conformational transitions that finally induce the gating process. An experimental examination of this gating model is in progress in our laboratory.

During the preparation of this manuscript, Paas et al. (1996b) published a mutational analysis of the chick kainate binding protein, a truncated nonmammalian homolog of glutamate receptor subunits of unknown function. Using equilibrium radioligand binding, they identified several agonist and antagonist binding residues, most of which lie at positions homologous to those implicated in glycine binding to the NR1 (Kuryatov et al., 1994; Hirai et al., 1996) and in glutamate binding to the NR2B (this study) subunits. Consequently, the overall structure of the LAOBP-based model of the kainate binding pocket presented by these authors shares several features with that of the NMDA receptor binding sites discussed here. However, the model of Paas et al. uses the closed rather than the open state of the bacterial protein as a structural template, i.e., a conformation likely to correspond to a desensitized rather than an activated receptor (Mano et al., 1996). Moreover, the interaction of agonists with the chick kainate binding protein differs significantly from that of glutamate with the NR2B subunit in that only nonionic polar side chains are suggested for ligand binding. Also, the conformation proposed for glutamate and kainate within the binding pocket of the chick kainate binding protein deviates from that predicted here and that inferred from medicinal chemistry (Chamberlin and Bridges, 1993; Shimamoto and Ohfune, 1996). Further comparison of the structures presented by Paas et al. (1996b) and in this study might highlight features relevant for agonist discrimination and the conformational transitions related to channel gating and inactivation.

In conclusion, our data possibly provide the first detailed molecular framework for understanding the glutamate binding site of the NMDA receptor. In addition, the comparative modeling approach described here allows predictions about the binding properties of its two principal agonist binding sites. Further exploitation of our models thus should foster the rational design of drugs that selectively target these sites and allow modulation

of NMDA receptor channel activity under physio- and pathological conditions.

Experimental Procedures

In Vitro Mutagenesis

Mutations were introduced into the NR2B (or ε2; see Kutsuwada et al., 1992) subunit cDNA by polymerase chain reaction using the following restriction fragments of plasmid pNR2B: 1.6 kb *Afl*II/*Cla*I for mutants E387A and F390S; 0.8 kb *Bst*EII for mutants K459A and H460F; 0.82 kb *Sph*I for mutants S486A, R493K, V660A, and S664G; and 0.64 kb *Bsm*I for mutants V709A and F731A. The redundancy of the genetic code was exploited to design primers for each mutant so as to introduce novel diagnostic restriction enzyme cleavage sites in the vicinity of the substitution. The resulting mutant cassettes were subcloned into the NR2B cDNA using the above-mentioned restriction sites and confirmed by DNA sequencing.

cRNA Synthesis and Oocyte Expression

*Not*I-linearized plasmid cDNAs were used for the in vitro synthesis of cRNA (mCAP mRNA Capping Kit, Stratagene, San Diego, CA) as described (Kuryatov et al., 1994). cRNAs of the rat clone pN60 (containing the NR1a cDNA; see Moriyoshi et al., 1991) and the mouse ε2 plasmid (containing the NR2B cDNA, see Kutsuwada et al., 1992) were synthesized using either T7 or T3 RNA polymerase, respectively. The isolation and maintenance of oocytes isolated from female Xenopus laevis anesthesized with urethane has been described previously (Schmieden et al., 1989; Kuryatov et al., 1994). cRNA concentrations were determined by both measuring optical densities at 260 nm and comparing staining intensities after gel electrophoresis. For oocyte injection, the concentrations of the cRNA samples were adjusted to 200–500 ng/μl, and appropriately diluted aliquots of the NR1a and NR2B cRNAs were mixed at a ratio of 1:3 (Laube et al., 1993). Microinjection of ≈50 nl cRNA into Xenopus laevis oocytes and voltage-clamp recording of agonist responses in Mg^{2+}-free frog Ringer's solution at a holding potential of −70 mV were performed as described (Schmieden et al., 1989; Laube et al., 1993).

Electrophysiological Analysis

Concentration-response curves for glycine and glutamate were generated by measuring the inward current response produced by increasing concentrations of one of the agonists in the presence of saturating concentrations of the other agonist (Kuryatov et al., 1994). Data from individual oocytes were analyzed by computing best-fit lines using the Hill equation, to obtain the concentration of agonist producing 50% receptor activation (EC_{50}). Concentration-inhibition curves for antagonists were determined by applying increasing antagonist concentrations in the presence of glutamate concentrations corresponding to the respective EC_{50} value and a saturating concentration of glycine (10 μM). For statistical analysis, data were converted to $\log_{10}$ values and subjected to a nonpaired Student's *t* test using the StatView program (Abacus Concepts Inc., Berkeley).

Molecular Modeling of Binding Pockets

The amino acid sequences of the mature GluR3, GluR6, NR1a, and NR2B proteins were aligned to maximize the similarities between these four proteins (M. S. and D. P. Hesson, unpublished data). A first comparison of this composite with LAOBP was made by employing published alignments (O'Hara et al., 1993; Kuryatov et al., 1994; Stern-Bach et al., 1994). Further adjustment of homologous regions was achieved manually with the overall aim of minimizing the differences between the regions defined by the structural core of LAOBP. Employing the final alignment shown partially in Figure 1, homology models of the agonist binding domains of the NR1 and NR2B subunits were constructed that are based on the known crystal structure of unliganded LAOBP (Oh et al., 1993). All models were made with the protein modeling package of "Quanta v4.0" (Molecular Simulations Inc.). Regions predicted to adopt a secondary structure homologous to LAOBP were modeled by duplicating those regions of the template protein. Sequences of the NR1 and NR2B proteins not included in the template structure were analyzed using standard algorithms for predicting protein secondary structure (Fasman, 1989). Utilizing the predicted propensity of these fragments to adopt helical, β-sheet, or turn geometries, these sequences were modeled further by comparison to a protein structural library and then annealed onto the existing structural framework. The complete structure was energetically minimized by initially holding the peptide backbone rigid (until root mean square difference <0.01), and then without constraints. The dielectric constant was set at 1.0; this value was found to be adequate to reduce reorganization of the protein backbone. Subsequently, the individual side chains were adjusted to remove unusual conformations, and the structure was again reminimized. Charged and polar side chains were manually adjusted to maximize pairing of H bonds and opposite charges followed by repeated minimization.

Modeling of Receptor–Ligand Complexes

Individual ligands were placed within close proximity (1–2 Å) of the presumed binding pocket, and then the receptor–ligand complex was energetically minimized without constraints. For each ligand, its conformation and orientation within the binding pocket was systematically adjusted, and the complex was reminimized. Only the lowest energy structure was retained after each iteration. This procedure resulted in models that represent an optimal fit of the ligand within the respective binding pocket.

Acknowledgments

This paper is dedicated to Jean-Pierre Changeux on the occasion of his 60th birthday. We thank D. Magalei for expert technical assistance, Drs. Robert Harvey and Stefan Boehm for critical reading of the manuscript, and M. Baier and H. Reitz for secretarial help. This work was supported by Deutsche Forschungsgemeinschaft (SFB 169) and Fonds der Chemischen Industrie. H. H. was supported by a postdoctoral fellowship from the Alexander-von-Humboldt Foundation.

Received January 20, 1997; revised February 18, 1997.

References

Arvola, M., and Keinänen, K. (1996). Characterization of the ligand-binding domains of glutamate receptor (GluR-B and GluR-D) subunits expressed in Escherichia coli as periplasmic proteins. J. Biol. Chem. *271*, 15527–15532.

Bennett, J.A., and Dingledine, R. (1995). Topology profile for a glutamate receptor: three transmembrane domains and a channel-lining reentrant membrane loop. Neuron *14*, 373–384.

Benveniste, M., and Mayer, M.L. (1991). Kinetic analysis of antagonist action at N-methyl-D-aspartic acid receptors. Two binding sites each for glutamate and glycine. Biophys. J. *59*, 560–573.

Chamberlin, R., and Bridges, R. (1993). Conformationally constrained acidic amino acids as probes of glutamate receptors and transporters. In Drug Design for Neuroscience, A. P. Kozikowski, ed. (New York: Raven Press, Ltd.).

Choi, D.W. (1988). Glutamate neurotoxicity and diseases of the nervous system. Neuron *1*, 623–634.

Clements, J.D., and Westbrook, G.L. (1991). Activation kinetics reveal the number of glutamate and glycine binding sites on the N-methyl-D-aspartate receptor. Neuron *7*, 605–613.

Durand, G.M., Gregor, P., Zheng, X., Bennett, M.V., Uhl, G.R., and Zukin, R.S. (1992). Cloning of an apparent splice variant of the rat N-methyl-D-aspartate receptor NMDAR1 with altered sensitivity to polyamines and activators of protein kinase C. Proc. Natl. Acad. Sci. USA *89*, 9359–9363.

Fasman, G.D. (1989). Prediction of Protein Structure and the Principles of Protein Conformation. (New York: Plenum Press).

Grimwood, S., Le Bourdellès, B., and Whiting, P.J. (1995). Recombinant human NMDA homomeric NMDAR1 receptors expressed in mammalian cells form a high affinity glycine antagonist binding site. J. Neurochem. *64*, 525–530.

Henderson, G., Johnson, J.W., and Ascher, P. (1990). Competitive antagonists and partial agonists at the glycine modulatory site of

the mouse N-methyl-D-aspartate receptor. J. Physiol. (Lond.) *430*, 189–212.

Hirai, H., Kirsch, J., Laube, B., Betz, H., and Kuhse, J. (1996). The glycine binding site of the N-methyl-D-aspartate receptor subunit NR1: identification of novel determinants of coagonist potentiation in the extracellular M3–M4 loop region. Proc. Natl. Acad. Sci. USA *93*, 6031–6036.

Hollmann, M., and Heinemann, S. (1994). Cloned glutamate receptors. Annu. Rev. Neurosci. *17*, 31–108.

Hollmann, M., Boulter, J., Maron, C., Beasley, L., Sullivan, J., Pecht, G., and Heinemann, S. (1993). Zinc potentiates agonist-induced currents at certain splice variants of the NMDA receptor. Neuron *10*, 943–954.

Johnson, J.W., and Ascher, P. (1987). Glycine potentiates the NMDA response in cultured mouse brain neurons. Nature *325*, 529–531.

Kang, C.-H., Shin, W.-C., Yamagata, Y., Gokcen, S., Ames, G.F.-L., and Kim, S.-H. (1991). Crystal structure for the lysine-, arginine-, ornithine-binding protein (LAO) from *Salmonella typhimurium* at 2.7-Å resolution. J. Biol. Chem. *266*, 23893–23899.

Kawamoto, S., Uchino, S., Hattori, S., Hamajima, K., Mishina, M., Nakajima-Iijima, S., and Okuda, K. (1995). Expression and characterization of the ζ1 subunit of the N-methyl-D-aspartate (NMDA) receptor channel in a baculovirus system. Mol. Brain Res. *30*, 137–148.

Kemp, J.A., and Leeson, P.D. (1993). The glycine site of the NMDA receptor: five years on. Trends Pharmacol. Sci. *14*, 20–25.

Kendrick, S.J., Lynch, D.R., and Pritchett, D.B. (1996). Characterization of glutamate binding sites in receptors assembled from transfected NMDA receptor subunits. J. Neurochem. *67*, 608–616.

Kleckner, N.W., and Dingledine, R. (1988). Requirement for glycine in activation of NMDA-receptors expressed in *Xenopus* oocytes. Science *241*, 835–837.

Kuner, T., Wollmuth, L.P., Karlin, A., Seeburg, P.H., and Sakmann, B. (1996). Structure of the NMDA receptor channel M2 segment inferred from the accessibility of substituted cysteines. Neuron *17*, 343–352.

Kuryatov, A., Laube, B., Betz, H., and Kuhse, J. (1994). Mutational analysis of the glycine-binding site of the NMDA receptor: structural similarity with bacterial amino acid-binding proteins. Neuron *12*, 1291–1300.

Kutsuwada, T., Kashiwabuchi, N., Mori, H., Sakimura, K., Kushiya, E., Araki, K., Meguro, H., Masaki, H., Kumanishi, T., Arakawa, M., and Mishina, M. (1992). Molecular diversity of the NMDA receptor channel. Nature *358*, 36–41.

Kuusinen, A., Arvola, M., and Keinänen, K. (1995). Molecular dissection of the agonist binding site of an AMPA receptor. EMBO J. *14*, 6327–6332.

Laube, B., Kuryatov, A., Kuhse, J., and Betz, H. (1993). Glycine-glutamate interactions at the NMDA receptor: role of cysteine residues. FEBS Lett. *335*, 331–334.

Laurie, D.J., and Seeburg, P.H. (1994). Ligand affinities at recombinant N-methyl-D-aspartate receptors depend on subunit composition. Eur. J. Pharmacol. *268*, 335–345.

Lynch, D.R., Anegawa, N.J., Verdoorn, T., and Pritchett, D.B. (1994). N-methyl-D-aspartate receptors: different subunit requirements for binding of glutamate antagonists, glycine antagonists, and channel-blocking agents. Mol. Pharmacol. *45*, 540–545.

Madison, D.V. (1991). Mechanisms underlying long-term potentiation of synaptic transmission. Annu. Rev. Neurosci. *14*, 379–397.

Mano, I., Lamed, Y., and Teichberg, V.I. (1996). A Venus flytrap mechanism for activation and desensitization of α-amino-3-hydroxy-5-methyl-4-isoxazole propionic acid receptors. J. Biol. Chem. *271*, 15299–15302.

Mayer, M.L., and Westbrook, G.L. (1987). Permeation and block of N-methyl-D-aspartic acid receptor channels by divalent cations in mouse cultured central neurones. J. Physiol. (Lond.) *394*, 501–527.

Mayer, M.L., Westbrook, G.L., and Guthrie, P.B. (1984). Voltage-dependent block by Mg^{2+} of NMDA responses in spinal cord neurones. Nature *309*, 261–263.

Mayer, M.L., Vycklicky, L., and Clements, J. (1989). Regulation of NMDA receptor desensitization in mouse hippocampal neurons by glycine. Nature *338*, 425–427.

McIlhinney, R.A.J., Molnár, E., Atack, J.R., and Whiting, P.J. (1996). Cell surface expression of the human *N*-methyl-D-aspartate receptor subunit 1a requires the co-expression of the NR2A subunit in transfected cells. Neuroscience *70*, 989–997.

Meguro, H., Mori, H., Araki, K., Kushiya, E., Kutsuwada, T., Yamazaki, M., Kumanishi, T., Arakawa, M., Sakimura, K., and Mishina, M. (1992). Functional characterization of a heteromeric NMDA receptor channel expressed from cloned cDNAs. Nature *357*, 70–74.

Monyer, H., Sprengel, R., Schoepfer, R., Herb, A., Higuchi, M., Lomeli, H., Burnashev, N., Sakmann, B., and Seeburg, P.H. (1992). Heteromeric NMDA receptors: molecular and functional distinction of subtypes. Science *256*, 1217–1221.

Moriyoshi, K., Masu, M., Ishii, T., Shigemoto, R., Mizuno, N., and Nakanishi, S. (1991). Molecular cloning and characterization of the rat NMDA receptor. Nature *354*, 31–37.

Nakanishi, S. (1992). Molecular diversity of glutamate receptors and implications for brain function. Science *258*, 597–603.

Nakanishi, N., Shneider, N.A., and Axel, R. (1990). A family of glutamate receptor genes: evidence for the formation of heteromultimeric receptors with distinct channel properties. Neuron *5*, 569–581.

Nakanishi, N., Axel, R., and Shneider, N.A. (1992). Alternative splicing generates functionally distinct N-methyl-D-aspartate receptors. Proc. Natl. Acad. Sci. USA *89*, 8552–8556.

Oh, B.H., Pandit, J., Kang, C.H., Nikaido, K., Gokcen, S., Ames, G.F.L., and Kim, S.H. (1993). Three-dimensional structures of the periplasmic lysine/arginine/ornithine-binding protein with and without a ligand. J. Biol. Chem. *268*, 11348–11355.

O'Hara, P.J., Sheppard, P.O., Thogersen, H., Venezia, D., Haldemann, B.A., McGrane, V., Houamed, K.M., Thomsen, C., Gilber, T.L., and Mulvihill, E.R. (1993). The ligand-binding domain in metabotropic glutamate receptors is related to bacterial periplasmic binding proteins. Neuron *11*, 41–52.

Olney, J.W. (1990). Excitotoxic amino acids and neuropsychiatric disorders. Annu. Rev. Pharmacol. Toxicol. *30*, 47–71.

Paas, Y., Devillers-Thiéry, A., Changeux, J.-P., Medevielle, F., and Teichberg, V. (1996a). Identification of an extracellular motif involved in the binding of guanine nucleotides by a glutamate receptor. EMBO J. *15*, 1548–1556.

Paas, Y., Eisenstein, M., Medevielle, F., Teichberg, V.I., and Devillers-Thiéry, A. (1996b). Identification of the amino acid subsets accounting for the ligand binding specificity of a glutamate receptor. Neuron *17*, 979–990.

Priestley, T., Laughton, P., Myers, J., Le Bourdellès, B., Kerby, J., and Whiting, P.J. (1995). Pharmacological properties of recombinant human NMDA receptors comprising NR1a/NR2A and NR1a/NR2B subunit assemblies expressed in permanently transfected mouse fibroblast cells. Mol. Pharmacol. *48*, 841–848.

Reynolds, I.J., Murphy, S.N., and Miller, R.J. (1987). ^{3}H-labeled MK-801 binding to the excitatory amino acid receptor complex from rat brain is enhanced by glycine. Proc. Natl. Acad. Sci. USA *84*, 7744–7748.

Schmieden, V., Grenningloh, G., Schofield, P.R., and Betz, H. (1989). Functional expression in *Xenopus* oocytes of the strychnine binding 48 kd subunit of the glycine receptor. EMBO J. *8*, 695–700.

Shimamoto, K., and Ohfune, Y. (1996). Syntheses and conformational analyses of glutamate analogs: 2-(2-carboxy-3-substituted-cyclopropyl)glycines as useful probes for excitatory amino acid receptors. J. Med. Chem. *39*, 407–423.

Stern-Bach, Y., Bettler, B., Hartley, M., Sheppard, P.O., O'Hara, J., and Heinemann, S.F. (1994). Agonist selectivity of glutamate receptors is specified by two domains structurally related to bacterial amino-acid binding proteins. Neuron *13*, 1345–1357.

Sugihara, H., Moriyoshi, K., Ishii, T., Masu, M., and Nakanishi, S. (1992). Structures and properties of seven isoforms of the NMDA receptor generated by alternative splicing. Biochem. Biophys. Res. Comm. *185*, 826–832.

Sullivan, J.M., Traynelis, S.F., Chen, H.S.V., Escobar, W., Heinemann, S.F., and Lipton, S.A. (1994). Identification of two cysteine residues that are required for redox modulation of the NMDA subtype of glutamate receptor. Neuron *13*, 929–936.

Uchino, S., Sakimura, K., Nagahari, K., and Mishina, M. (1992). Mutations in a putative agonist binding region of the AMPA-selective glutamate receptor channel. FEBS Lett. *308*, 253–257.

Wafford, K.A., Kathoria, M., Bain, C.J., Marshall, G., Le Bourdellès, B., Kemp, J.A., and Whiting, P.J. (1995). Identification of amino acids in the *N*-methyl-D-aspartate receptor NR1 subunit that contribute to the glycine binding site. Mol. Pharmacol. *47*, 374–380.

Wo, Z.G., and Oswald, E. (1994). Transmembrane topology of two kainate receptors revealed by N-glycosylation. Proc. Natl. Acad. Sci. USA *91*, 7154–7158.

Wo, Z.G., and Oswald, E. (1995). Unraveling the modular design of glutamate-gated ion channels. Trends Neurosci. *18*, 161–168.

Zheng, X., Zhang, L., Durand, G.M., Bennett, M.V., and Zukin, R.S. (1994). Mutagenesis rescues spermine and Zn^{2+} potentiation of recombinant NMDA receptors. Neuron *12*, 811–818.